



LYAPUNOV EXPONENTS AND ADAPTIVE MESH REFINEMENT FOR HIGH-SPEED FLOWS

Rodrigo Costa Moura
 André Fernando de Castro da Silva
 Aline Sousa da Silveira
 Marcos Aurélio Ortega

Technological Institute of Aeronautics - ITA, São José dos Campos, Brazil
 moura@ita.br, andref@ita.br, aline.s.silveira@gmail.com, ortega@ita.br

Abstract. *When dealing with high-speed flows, within the transonic, supersonic or hypersonic regimes, the presence of shock-wave phenomena dictates the main features of the flow. Shock waves are very thin structures across which the flow properties vary in a practically discontinuous fashion. Therefore, within the environment of computational fluid dynamics, the employment of adaptive mesh refinement is crucial for the proper capturing of shock waves and related flow transitions. This work presents an elegant approach for the precise demarcation of shocks, minding the subsequent application of local grid refinement. The proposed technique is based on the use of an operator originally developed within the context of dynamical systems, namely, the Finite Time Lyapunov Exponent (FTLE). When applied to the dilatation field (divergence of velocity) of the flow, such operation is capable of highlighting shock-waves in a remarkable way. In order to demonstrate the capabilities of the method, different test cases are addressed, minding specially the aerospace context.*

Keywords: *Adaptive mesh refinement, Finite Time Lyapunov Exponent, Shock waves, CFD*

1. INTRODUCTION

The physical phenomena that take place in high-speed flows is of paramount importance specially in the aerospace context. For such flows, the presence of structures known as shock waves, through which the fluid properties experience an abrupt change, dictates the main features of the flow field. In typical aeronautical conditions, the thickness of a shock wave is so small (about 10^{-7} m) that it may be regarded as a discontinuity. This feature represents an extremely difficult challenge for numerical schemes which are designed to simulate such flows.

When a numerical scheme is used to solve a set of partial differential equations (PDE) modeling the physical phenomena taking place, a discrete domain is chosen where an algebraic approximation to the PDEs is actually solved. Regardless of the numerical formulation adopted, the local error and hence the accuracy of the solution are functions of the local mesh size. In the vicinity of shocks, numerical schemes normally introduce unphysical wiggles, commonly related to the Gibbs' phenomenon. The methodologies developed to overcome this issue usually reduce the local accuracy to first order in these regions, smearing the shock waves and increasing the associated numerical thickness. In such cases, only a local mesh refinement would diminish the numerical dissipation and provide a better shock resolution without the excessive computational cost that would follow from global mesh refinement.

Thus, the use of local mesh refinement has become a very useful tool when dealing with high speed flows and has drawn the interest of the scientific community (Arney and Flaherty, 1989). In the past 30 years there was plenty of works which addressed several algorithms and convergence efficiency studies that proved the importance of such tool (Rheinboldt, 1980; Berger and Collela, 1989; Berger and Olinger, 1984). Many of them use a multigrid-like approach consisting of using several layers of progressively refined meshes that are overlaid only in the regions where the refinement is needed. The main advantage of such approaches is that there is no change in the main mesh being calculated, which is very interesting specially when dealing with complex geometries. In this work, however, it was adopted a different approach similar to the work of Ripley *et al.* (2004), in which the initial mesh is subjected to an iterative process where successive refinements based in preliminary solutions obtained in the coarser grids are performed.

One of the most fundamental issues to be addressed when performing an adaptive mesh refinement is to determine the regions which need to be subjected to the procedure, i.e. the locations of large gradients. In this paper, an operator originally developed within the context of dynamical systems, namely, the Finite Time Lyapunov Exponent (FTLE) is used to perform this task. An in depth analysis of the FTLE operator and of its applications is given in the work of Shadden *et al.* (2005). Therefore, there is no need to reproduce all those details here.

This paper is organized as follows. A brief introduction to the FTLE operator is presented in section 2. The main aspects concerning the refinement procedure are addressed in section 3. The numerical formulation of the solver used for the simulations addressed, along with the test cases of interest, is described in section 4. Final comments and future research possibilities are discussed in section 5.

2. THE FINITE TIME LYAPUNOV EXPONENT

Recently, the development of the dynamical systems theory (specially in the field of non-linear dynamics and chaos) and its application in fluid dynamics has provided interesting insights on the physics of a variety of flows using the so called Lagrangian approach to the problem (Franco *et al.*, 2007; Cardwell and Mohseni, 2007; Salman *et al.*, 2007). As opposed to the Eulerian scheme, the attention is here focused on the movement of each individual particle of fluid.

It is known that even unsteady flows may admit material lines which have an attractive or repulsive character with regard to the fluid particles (Haller, 2001). Specially, following Shadden *et al.* (2005), the material lines derived from individual particle trajectories are called Lagrangian Coherent Structures (LCS). A stable LCS is defined as the locus of points whose trajectories converge to a particular region when $t \rightarrow \infty$ (forward integration). Analogously, an unstable LCS is the locus of points whose trajectories converge to a particular region when $t \rightarrow -\infty$ (backward integration).

Shadden *et al.* (2005) have demonstrated that the LCSs can be calculated using the FTLE operator. Specifically, one can show that the LCSs correspond to the ridges of the scalar field calculated by the FTLE. These ridges can be understood as attracting (or repelling) structures whose dimensionality corresponds to the considered flow dimension subtracted by one. For the two-dimensional flows of interest in the present research, the calculated LCSs are curves representing shock waves.

2.1 Calculation methodology

Basically, the FTLE is a measure of the local repulsion (or attraction) of neighbor particles traveling on a given flow field. In practice, it can be defined as the time-averaged maximum exponential rate of repulsion between particles initially very close. Such particles must be convected by a prescribed vector field during a suitable time interval.

Let $\phi_{t_0}^{t_0+T}(x, y)$ be the position vector at time $t_0 + T$ of a particle that, in time t_0 , occupies the position (x, y) and let $\delta_i = (\delta x, \delta y)$ be an infinitesimal vector pointing toward an arbitrary direction. The initial difference δ_i between the positions of two close particles will be amplified to the final distance $\delta_f = \phi_{t_0}^{t_0+T}(x + \delta x, y + \delta y) - \phi_{t_0}^{t_0+T}(x, y)$ by the "traveling" function ϕ after a time interval T . Note that positive values of T correspond to a forward integration of the particles trajectories in time and a negative value of T correspond to a backward integration in time. The FTLE value calculated at (x, y) , denoted by $\sigma_{t_0}^T(x, y)$, is given by

$$\sigma_{t_0}^T(x, y) = \max_{\delta_i} \frac{1}{T} \ln \left(\frac{|\delta_f|}{|\delta_i|} \right), \quad (1)$$

where δ_i is allowed to vary within a close perimeter of neighbor particles in order to provide the maximum local repulsion rate.

Note that, once the parameters t_0 and T are chosen, $\sigma_{t_0}^T(x, y)$ is a function of the position $\mathbf{p} = (x, y)$ only and therefore represents a scalar field. Numerically, an efficient way to calculate this quantity over a entire domain was proposed by Padberg *et al.* (2007). The key idea is to generate an equally-spaced Cartesian mesh whose nodes represent the initial position of particles. Then, one can evaluate, for every grid node, the value of $\phi_{t_0}^{t_0+T}(x, y)$ by integrating the trajectories of each node-related particle. For sufficiently refined grids, the FTLE can be approximated by

$$\sigma_{t_0}^T(\mathbf{p}) = \frac{1}{|T|} \ln \left(\max_j \frac{|\phi_{t_0}^{t_0+T}(\mathbf{p}) - \phi_{t_0}^{t_0+T}(\mathbf{n}_j(\mathbf{p}))|}{|\mathbf{p} - \mathbf{n}_j(\mathbf{p})|} \right), \quad (2)$$

where $\mathbf{n}_j(\mathbf{p})$ represents each of the eight mesh positions that are closest to \mathbf{p} , namely, the satellite particles presented in Fig. 1. Note that the term $\phi_{t_0}^{t_0+T}(\mathbf{n}_j(\mathbf{p}))$ represent the position of each of the satellite particles at the end of the time interval T . This expression is preferable when compared to other ones available in the literature because it avoids the numerical calculation of derivatives. The finer the mesh used to calculate the FTLE, the more accurate will be the resulting scalar field.

Note that according to the LCS definition previously presented, a high local value of the FTLE scalar field for either a positive T (progressive integration) or negative T (regressive integration) would correspond to LCSs. Actually, it can be shown (Shadden *et al.*, 2005) that one distinctive feature of the resulting scalar field is that it presents a constant value at the LCSs and a null value elsewhere. This property will play a fundamental role in the present work since the shock regions are intended to be equally demarcated regardless of the shock strength.

2.2 The velocity field analogy

As previously stated in the introduction, a major issue regarding the refinement process is to determine the regions where the abrupt variation of the fluid properties requires a finer mesh in order to achieve a better local accuracy.

Several shock sensors have already been proposed in the literature for a wide range of numerical methods. In the present work the dilatation field (velocity divergence) was adopted following the works of Bhagatwala and Lele (2009)

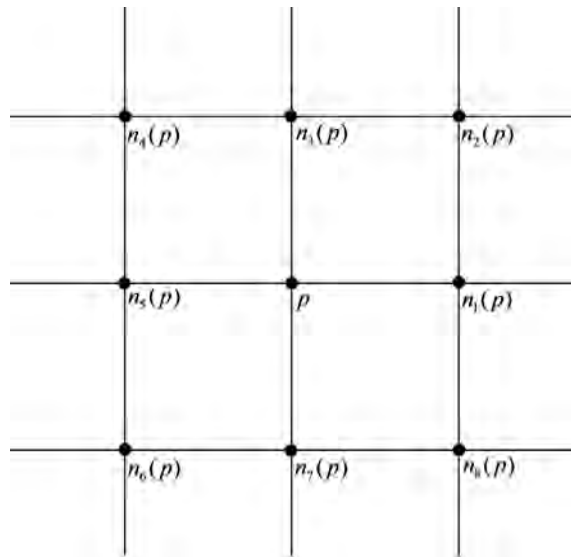


Figure 1. Schematic illustration for the calculation of the FTLE showing a target node and its satellite nodes.

and Premasathan *et al.* (2010), since such variable reaches strong negative values at shock waves. Actually, shock waves correspond to ridges of negative magnitude in the dilatation field.

It is now useful to imagine a velocity field given by the dilatation gradient vector field. The shock wave will act as a repulsive structure to particles following this velocity field since the gradient vector will point to opposite directions on each side of the shock wave. Thus, the FTLE based on progressive integration will provide a maximum value along the entire shock wave. Obviously, the finer the mesh used to evaluate the FTLE, the better will be the resolution of the shock location but also the more expensive will be the calculation. Figure 2 shows the dilatation field close to the shock wave ahead a circular cylinder subjected to a supersonic flow. The dilatation gradient field is represented by the black arrows. Note that particles following such (virtual) velocity field would be repelled away from each other depending on which side of the shock wave they are placed initially.

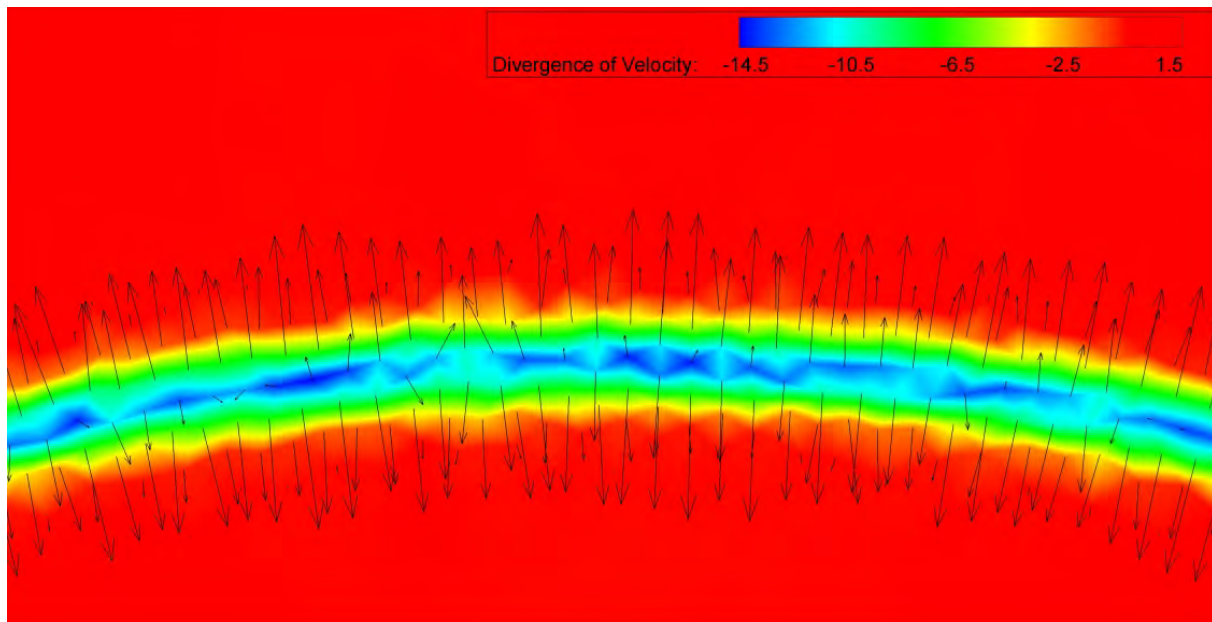


Figure 2. Dilatation field of the shock wave ahead a circular cylinder subjected to a Mach-2.5 uniform flow. The vectors represent the velocity field that (virtual) particles would follow according with the proposed analogy.

3. THE REFINEMENT PROCEDURE

Having in mind complex geometries, the use of unstructured meshes is a logical choice. They were created using the software *Distmesh* (Persson and Strang, 2004), a Matlab[®] code developed by Persson (2005). This subroutine is able

to generate unstructured meshes for geometries specified via implicit functions, iteratively improving an initial mesh by enforcing an equilibrium of forces at the element edges. It uses three basic inputs to generate any triangular mesh:

- The minimum mesh length h_0 ;
- A scalar field $f_d(x, y)$ that corresponds to the distance of point (x, y) to the closest boundary, yielding a negative value for points inside the domain and a positive value outside of it;
- The element size function $f_h(x, y)$ that corresponds to the relative local mesh length scaled by h_0 .

The function $f_d(x, y)$ is solely settled by the domain boundary geometry and, therefore, only needs to be determined once. The minimum mesh length h_0 is a global measure of the mesh coarseness and the principal parameter to be changed in a mesh convergence analysis. Thus, the main objective here is to determine the element size function $f_h(x, y)$ so that the vicinities of the shock waves are refined.

The mesh refinement procedure is based on an iterative process that follows basically four steps as illustrated by Fig. 3. Beginning with a initial mesh which does not present any specific refinement besides that needed to provide a better description of the boundary conditions, the first step is to use a numerical solver to calculate the solution which represents a preliminary approximation to the desired flow pattern. In the second step, the flow properties, represented by the elements averages stored at the triangles barycenters, are interpolated to an auxiliary equally-spaced Cartesian mesh, in which all further calculations will take place (the finer the mesh, the more accurate the following calculations will be).

The velocity divergence field is then calculated and the FTLE operator can be used to determine the shock waves location as the set of nodes (in the auxiliary mesh) whose calculated FTLE value exceeds a suitable cutoff value. A new element size function $f_h^i(x, y)$ is obtained based on the radial distance of any point (x, y) to the position of the marked shock-related nodes. A new mesh is then generated using the *Distmesh* and the entire procedure is repeated until the shock waves are sufficiently resolved in the numerical solution.

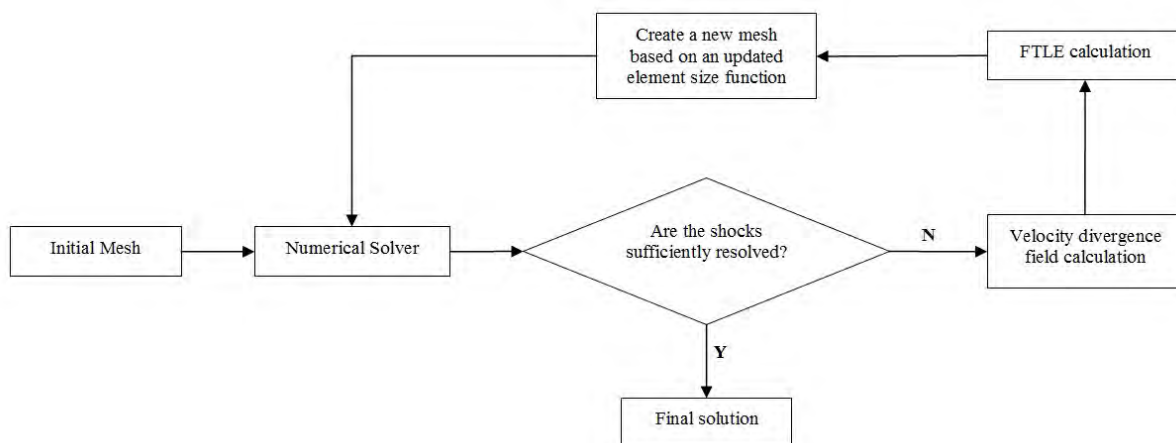


Figure 3. Schematic illustration showing the major steps of the refinement procedure.

It is worth mentioning that the initial mesh needs to have a minimum degree of refinement in order to provide good results for the first shock demarcations. Since the shock location may slightly change between successive iterations due to the coarseness of the intermediary meshes, it is advisable to perform a few steps of progressive refinement instead of a single one.

4. NUMERICAL RESULTS

In order to verify the capabilities of the proposed methodologies, a numerical solver to the Euler equations of gas dynamics was used to simulate the physics of inviscid compressible air flows. The code is based on the Discontinuous Galerkin (DG) scheme for unstructured meshes. In the solver here use, the treatment of shocks can be performed by means of artificial viscosity approaches or via an ENO-based limiting technique. The reader is referred to the works of Moura (2012) and Silva (2012) for a detailed description of the DG formulation and of the shock-capturing approaches available in the code. For the present research, the element-wise constant artificial viscosity model due to Person and Peraire (2006) is employed. In addition, the high-order treatment of curved boundaries follows the work of Sevilla *et al.* (2008), see also the report due to Moura and Silveira (2013) for implementation details.

Three test cases were chosen to demonstrate the refinement procedure proposed in section 3, namely, a transonic airfoil, the supersonic flow past a circular cylinder and the forward facing step in a supersonic channel. All results were

obtained with a polynomial order of 2 (which yields a third-order spatial accuracy at smooth regions), and with the inviscid Lax-Friedrichs (Rider and Lowrie, 2002) and the viscous BR2 (Bassi *et al.*, 1997; Brezzi *et al.*, 2000) numerical fluxes. It is important to say that the refinement methodology here proposed can be used as well with classical low-order formulations.

4.1 The transonic flow over a NACA-0012 airfoil (cutoff analysis)

The first test case is the transonic flow past a standard NACA-0012 airfoil with sharp trailing edge. The chosen freestream Mach number is 0.80 and the angle of attack is set to 1.50 degrees. The flow is solved within a circular domain centered at the profile with a far-field outer diameter of 20 chords. Figure 4(a) shows a global view of the initial mesh used for the refinement procedure. Each individual mesh thereafter will only differ on the near-shock refinement pattern.

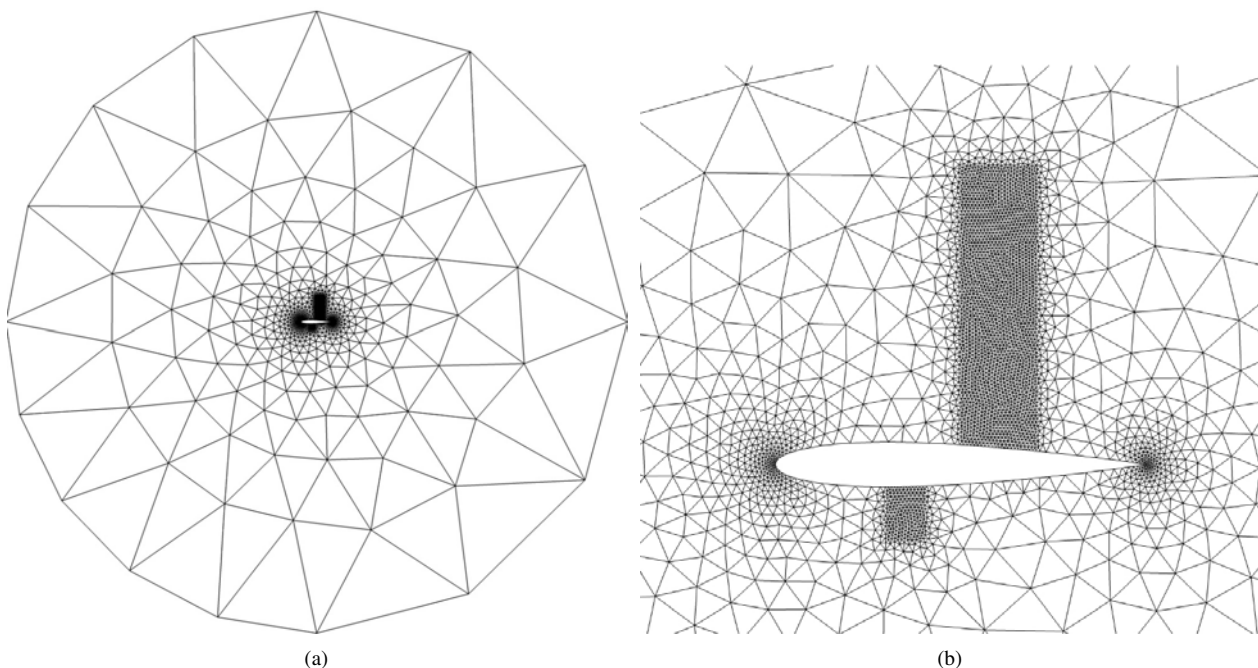


Figure 4. The chosen mesh for the cutoff analysis: (a) A global overview of the mesh used in the NACA-0012 transonic simulations. (b) A closer look showing a block-shaped refined region in the mesh used for the cutoff analysis.

Probably the first thing someone might argue is that it is easier to use the dilatation field directly to build the element size function. In order to address this issue, a block-like refinement was performed in the regions enclosing the shock wave in the upper surface and the weaker one in the lower surface. The element sizing for both regions is uniform and the value of h_0 is the same. Note that the stronger the shock wave, the bigger the dilatation absolute value at that point. Thus, to use the dilatation field directly would lead to a stronger refinement in the upper surface.

In order to compare the efficiency of both the dilatation field and the FTLE to determine the location of the shock waves, the scalar fields were normalized by its maximum values. A point is said to belong to a shock wave if the normalized scalar field value at that point is larger than an adjustable cutoff value. The right side of Fig. 5 highlights the grid nodes that are marked by the FTLE as belonging to the shock wave for a given cutoff value; and the left side shows the grid nodes that were marked by the dilatation field for the cutoff value that provide the same number of point marked by the FTLE. Note that for the same number of grid nodes, the FTLE is capable of marking a longer extension of the upper shock wave or even capture the lower surface shock wave when the dilatation field alone is not capable of.

Using the nodes previously marked by the FTLE, one can create the refined mesh presented in Fig. 6(a) and calculate the flow past the profile one more time. The resulting Mach number field is presented in Fig. 6(b).

4.2 The supersonic flow past a circular cylinder

The second test case is the supersonic flow past a circular cylinder. The incident flow is directed downwards and has a freestream Mach number of 2.5. Following the refinement steps presented in section 3, three complete cycles were performed. Figure 7 presents all meshes created throughout the process. An interesting feature of these meshes is the fact that the refinement degree is the same along the entire shock extension. This results from the FTLE property of delivering a constant value along the shock wave no matter how strong it is. Other methodologies tend to furnish a stronger refinement near the stagnation point where the shock transition is stronger so that the numerical results tend to

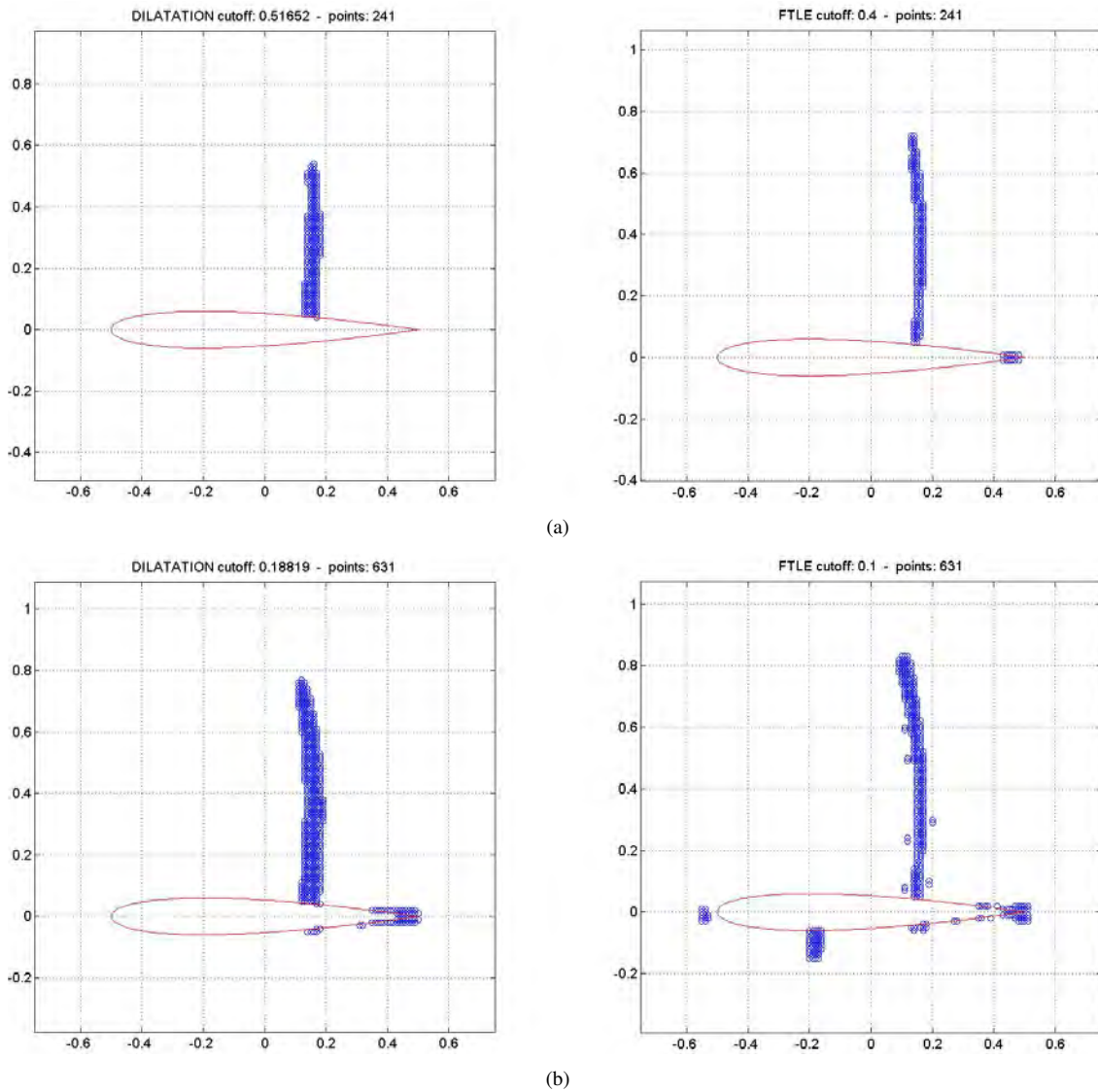


Figure 5. The illustrations show the node positions which are marked for refinement using simply the dilatation field (left) and the corresponding FTLE based on the dilatation field (right) for the same number of marked points: (a) Using a cutoff of 40% of the maximum FTLE field magnitude. (b) Using a cutoff of 10% of the maximum FTLE field magnitude.

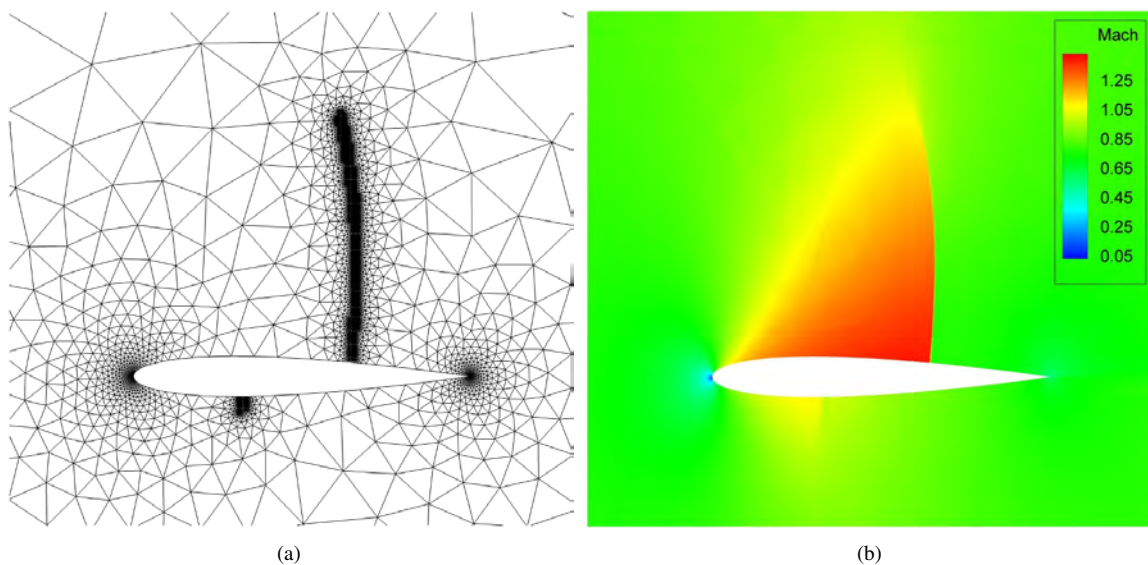


Figure 6. The final solution: (a) The final used mesh; (b) The final Mach number field.

display an increasing smearing of the shock wave away from the symmetry line. The successive solutions for both Mach number and static pressure are presented in Fig. 8, where an expressive improvement in the shock resolution is achieved by efficiently employing the refinement only along the shock wave.

4.3 The steady supersonic flow through a channel with a forward facing step

The third and last test case is a modification of the classical forward facing step problem by Woodward and Colella (1984). The solution domain is two units high in the inlet section and six units long. The relative step height was modified from 20% to 17.5% so that the problem admits a steady-state solution. For all cases the inlet Mach number is set to be 3.

The initial mesh is essentially uniformly spaced with only a local refinement near the geometric discontinuity represented by the step, as presented in Fig. 9(a). Figures 9(b) and 9(c) show, respectively, the velocity divergence and the Mach number fields simulated in this initial Mesh. After 7 refinement cycles, the final mesh obtained is the one presented in Fig. 10(a). The corresponding velocity divergence and Mach number fields, showed in Figs. 10(b) and 10(c), attest the quality of the FTLE-based refinement procedure. Again, one can see that the shock waves were equally refined along their entire extension despite their different local intensity.

5. CONCLUSIONS

This article presented a new methodology to perform adaptive mesh refinement focused on shock capturing that is based on a dynamical systems operator named Finite Time Lyapunov Exponent (FTLE). After a brief introduction to the fundamental concepts regarding the FTLE, a velocity field analogy was formulated that allowed the calculation of the shock waves location by applying the FTLE operator to the gradient of the dilatation field (divergence of the velocity). This procedure has shown to be more efficient in marking the shock location when compared to the direct use of the dilatation field, since a narrower number of points is used to represent the discontinuity.

Numerical tests were presented that not only demonstrated the methodology efficiency but also the quality of the resulting simulations. Due to the outstanding mathematical properties of the FTLE operator, the entire extension along the shock waves is almost equally refined despite the local shock intensity which grants a uniformly sharp shock transition throughout its entire extension.

Among future research possibilities, one can mention the extension to three-dimensional geometries and unsteady flows. Moreover, a more accurate interpolation procedure can be devised, "between" the actual mesh and the auxiliary mesh used to perform the shock location calculations, by using the high-order information from the polynomials within each element. At last, an advanced methodology can be developed to automatically perform the iteration steps which are currently carried out manually.

6. ACKNOWLEDGMENTS

The authors gratefully acknowledge the support for this research provided by FAPESP (Sao Paulo Research Foundation), under the Research Grant No. 2012/16973-5.

7. REFERENCES

- Arney, D. and Flaherty, J., 1989. "An adaptive local mesh refinement method for time-dependent partial differential equations". *Applied Numerical Mathematics*, Vol. 5, pp. 257–274.
- Bassi, F., Rebay, S., Mariotti, G., Pedinotti, S. and Savini, M., 1997. "A high-order accurate discontinuous finite element method for inviscid and viscous turbomachinery flows". In *Proceedings of the 2nd European Conference on Turbomachinery Fluid Dynamics and Thermodynamics*. Antwerp, Belgium.
- Berger, M. and Colella, P., 1989. "Local adaptive mesh refinement for shock hydrodynamics". *Journal of Computational Physics*, Vol. 82, pp. 64–84.
- Berger, M. and Olinger, J., 1984. "Adaptive mesh refinement for hyperbolic partial differential equations". *Journal of Computational Physics*, Vol. 53, pp. 484–512.
- Bhagatwala, A. and Lele, S., 2009. "A modified artificial viscosity approach for compressible turbulence simulations". *Journal of Computational Physics*, Vol. 14, No. 228, pp. 4965–4969.
- Brezzi, F., Manzini, G., Marini, L., Pietra, P. and Russo, A., 2000. "Discontinuous Galerkin approximations for elliptic problems". *Numerical Methods for Partial Differential Equations*, Vol. 16, pp. 365–378.
- Cardwell, B. and Mohseni, K., 2007. "A Lagrangian view of vortex shedding and reattachment behavior in the wake of a 2D airfoil". In *Proceedings of the 37th AIAA Fluid Dynamics Conference and Exhibit*. Miami, FL.
- Franco, E., Pekarek, D., Peng, J. and Dabiri, J., 2007. "Geometry of unsteady fluid transport during fluid-structure interactions". *Journal of Fluid Mechanics*, Vol. 589, pp. 125–145.
- Haller, G., 2001. "Distinguished material surfaces and coherent structures in three-dimensional fluid flow". *Physica D:*

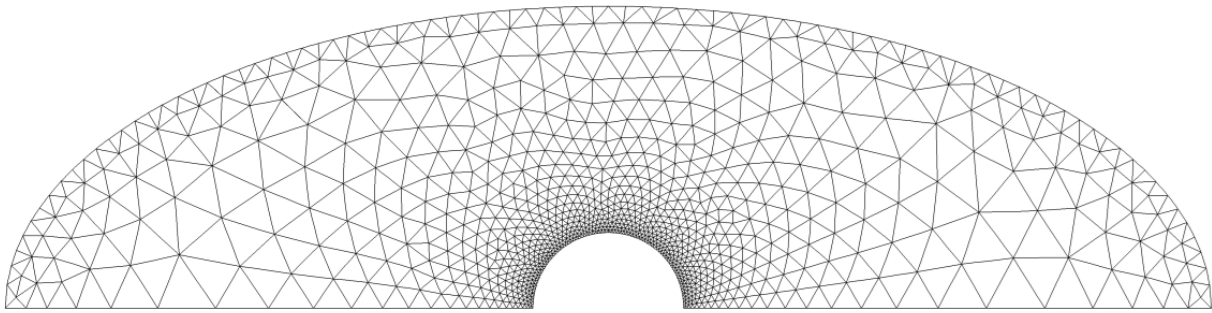
Moura R.C., Silva A.F.C., Ortega M.A. and Silveira A.S.
Lyapunov Exponents and Adaptive Mesh Refinement for High-Speed Flows

Nonlinear Phenomena, Vol. 149, No. 4, pp. 248–277.

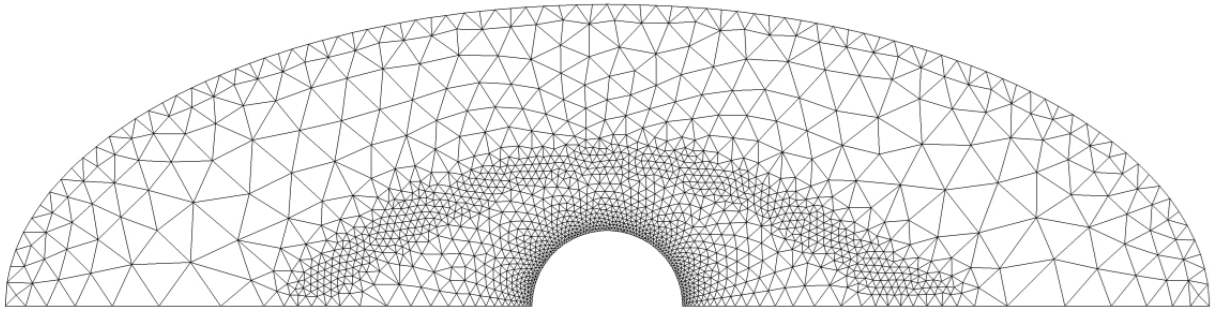
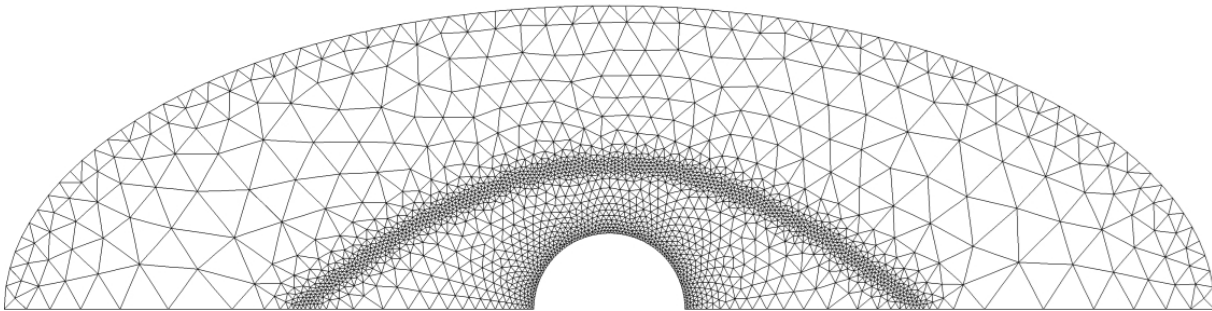
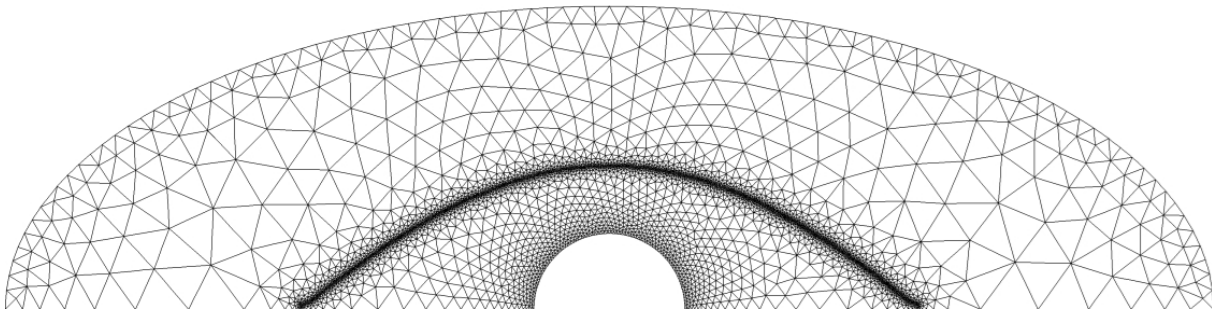
- Moura, R.C., 2012. *A high-order unstructured discontinuous Galerkin finite element method for aerodynamics*. Division of Aeronautics Engineering, Aeronautics Institute of Technology, Thesis (Masters in Sciences in Aeronautical and Mechanics Engineering).
- Moura, R. and Silveira, A., 2013. “O tratamento de fronteiras curvas no código Veritas2D”. LASCAs report (unpublished), Technological Institute of Aeronautics, São José dos Campos, Brazil.
- Padberg, K., Hauff, T., Jenko, F. and Junge, O., 2007. “Lagrangian structures and transport in turbulent magnetized plasmas”. *New Journal of Physics*, Vol. 9, No. 11, pp. 400–415.
- Person, P.O. and Peraire, J., 2006. “Sub-cell shock capturing for discontinuous Galerkin methods”. In *Proceedings of the 44th AIAA Aerospace Sciences Meeting*. AIAA paper 2006-112.
- Persson, P.O., 2005. *Mesh Generation for Implicit Geometries*. Ph.D. thesis, Massachusetts Institute of Technology, Cambridge, USA.
- Persson, P.O. and Strang, G., 2004. “A simple mesh generator in Matlab”. *SIAM Review*, Vol. 46, No. 2, pp. 329–345.
- Premasuthan, S., Liang, C. and Jameson, A., 2010. “Computation of flows with shocks using spectral difference scheme with artificial viscosity”. In *Proceedings of the 48th AIAA Aerospace Sciences Meeting and Exhibit*. Orlando, Florida, AIAA Paper 2010-1449.
- Rheinboldt, W.C., 1980. “On a theory of mesh-refinement processes”. *SIAM Journal of Numerical Analysis*, Vol. 17, No. 6.
- Rider, W. and Lowrie, R., 2002. “The use of classical Lax-Friedrichs Riemann solvers with discontinuous Galerkin methods”. *International Journal for Numerical Methods in Fluids*, Vol. 40, pp. 479–486.
- Ripley, R., Lien, F.S. and Yovanovich, M., 2004. “Adaptive unstructured mesh refinement of supersonic channel flows”. *International Journal of Computational Fluid Dynamics*, Vol. 18, No. 2, pp. 189–198.
- Salman, H., Hesthaven, J. and Warburton, T., 2007. “Predicting transport by Lagrangian coherent structures with a high-order method”. *Theor. Comput. Fluid Dyn.*, Vol. 21, pp. 39–58.
- Sevilla, R., Fernández-Mendez, S. and Huerta, A., 2008. “NURBS-enhanced finite element method for Euler equations”. *International Journal for Numerical Methods in Fluids*, Vol. 57, pp. 1051–1069.
- Shadden, S., Lekien, F. and Marsden, J., 2005. “Definition and properties of Lagrangian coherent structures from finite-time Lyapunov exponents in two-dimensional aperiodic flows”. *Physica D: Nonlinear Phenomena*, Vol. 212, No. 3-4, pp. 271–304.
- Silva, A.F.C., 2012. *On the use of ENO-based limiters for discontinuous Galerkin methods for aerodynamics*. Division of Aeronautics Engineering, Aeronautics Institute of Technology, Thesis (Masters in Sciences in Aeronautical and Mechanics Engineering).
- Woodward, P. and Colella, P., 1984. “The numerical simulation of two-dimensional fluid flow with strong shocks”. *Journal of Computational Physics*, Vol. 54, pp. 115–173.

8. RESPONSIBILITY NOTICE

The authors are the only responsible for the printed material included in this paper.



(a) Initial mesh.

(b) 1st iteration.(c) 2nd iteration.

(d) Final mesh.

Figure 7. Set of meshes corresponding to successive iterations of the refinement procedure.

Moura R.C., Silva A.F.C., Ortega M.A. and Silveira A.S.
Lyapunov Exponents and Adaptive Mesh Refinement for High-Speed Flows

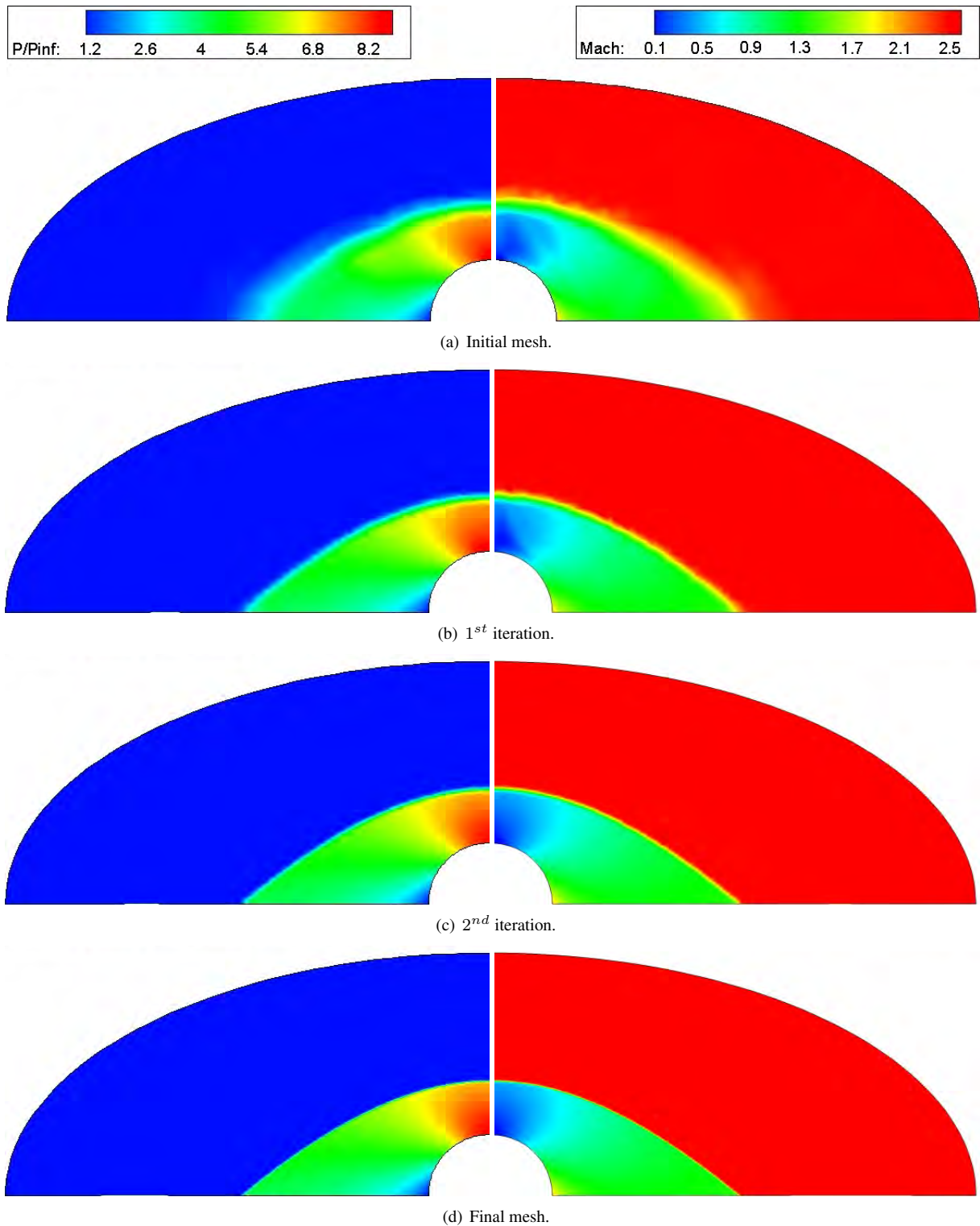
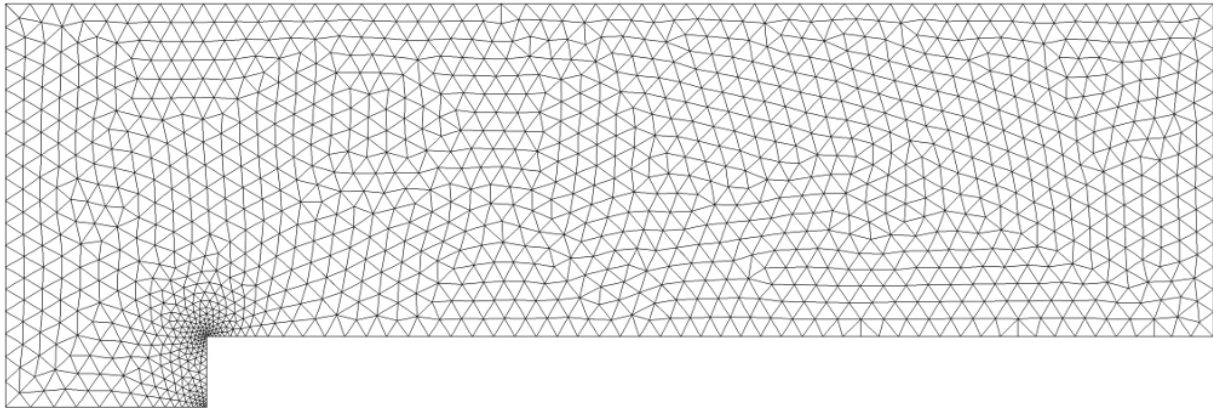
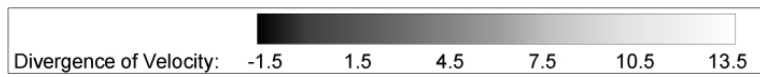


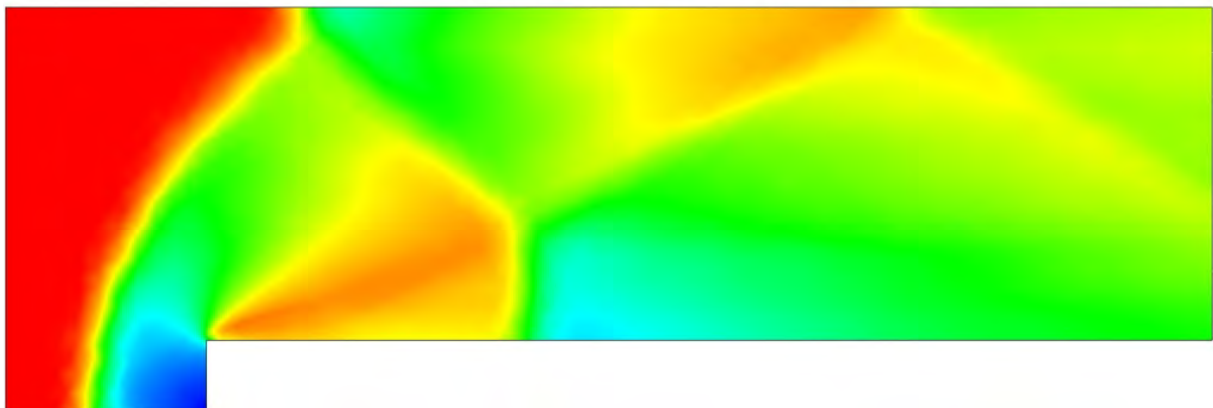
Figure 8. Static pressure (left) and Mach number (right) fields for successive iterations of the refinement procedure (corresponding to the meshes presented in Fig. 7).



(a) Initial mesh.



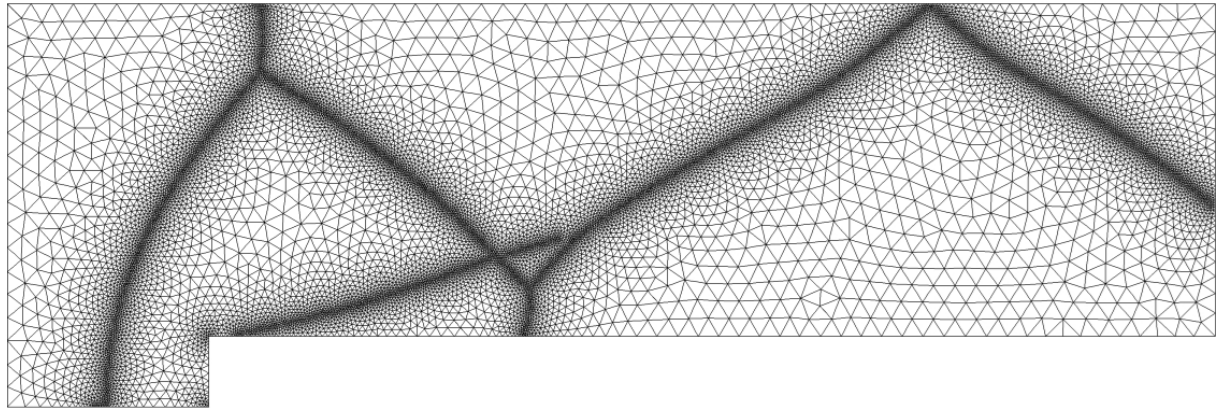
(b) Dilatation field.



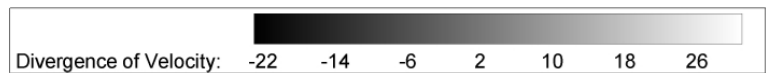
(c) Mach number field.

Figure 9. Initial mesh and solution for the forward facing step.

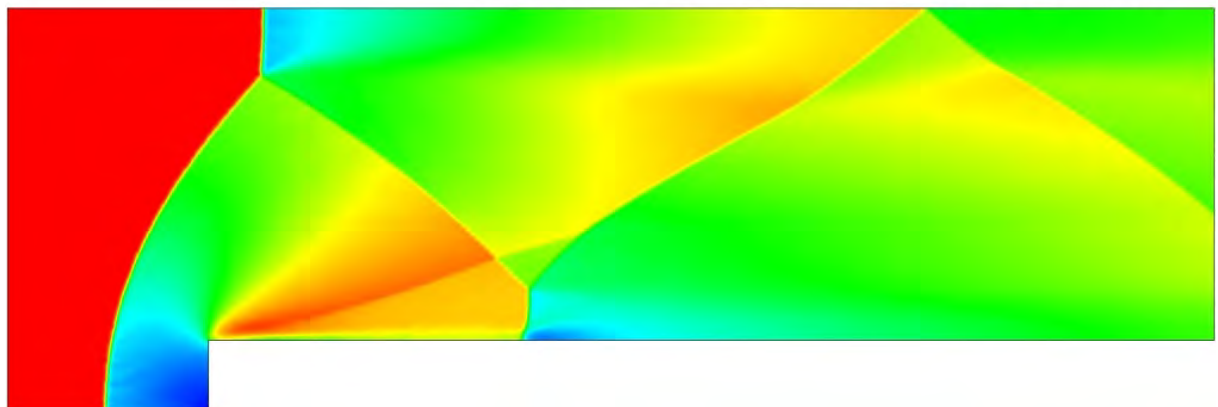
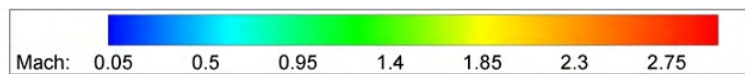
Moura R.C., Silva A.F.C., Ortega M.A. and Silveira A.S.
 Lyapunov Exponents and Adaptive Mesh Refinement for High-Speed Flows



(a) Final mesh.



(b) Dilatation Field.



(c) Mach number field.

Figure 10. Final mesh and solution for the forward facing step after 7 iterations.